



Article

Effect of Harvest Age on Total Phenolic, Total Anthocyanin Content, Bioactive Antioxidant Capacity and Antiproliferation of Black and White Glutinous Rice Sprouts

Visessakseth So ¹, Piman Pocasap ^{2,3} , Khaetthareeya Sutthanut ^{2,3}, Benjabhorn Sethabouppha ⁴, Wipawee Thukhammee ^{3,5}, Jintanaporn Wattanathorn ^{3,5} and Natthida Weerapreeyakul ^{2,3,*} 

¹ Graduate School (in the program of Pharmaceutical Sciences), Faculty of Pharmaceutical Sciences, Khon Kaen University, Khon Kaen 40002, Thailand; sovisessakseth@kkumail.com

² Division of Pharmaceutical Chemistry, Faculty of Pharmaceutical Sciences, Khon Kaen University, Khon Kaen 40002, Thailand; piman.pocasap@kkumail.com (P.P.); khaesu@kku.ac.th (K.S.);

³ Human High Performance and Health Promotion Research Institute, Khon Kaen University, Khon Kaen 40002, Thailand; wipath@kku.ac.th (W.T.); jinwat@kku.ac.th (J.W.)

⁴ Faculty of Pharmaceutical Sciences, Ubon Ratchathani University, Ubon Ratchathani 34190, Thailand; benjabhorn.s@ubu.ac.th

⁵ Department of Physiology, Faculty of Medicine, Khon Kaen University, Khon Kaen 40002, Thailand

* Correspondence: natthida@kku.ac.th; Tel.: +66-4320-2378

Received: 7 September 2020; Accepted: 4 October 2020; Published: 11 October 2020



Abstract: Black (cv. BGR) and white (cv. RD6) glutinous rice sprouts from fertilizer- and pesticide-free farm in Khon Kaen province, Thailand were investigated for antioxidation and antiproliferative activity. Three different ages of rice sprouts were collected and prepared as the extract. BGR exerted higher antioxidant capacity than RD6 based on total phenolic (TPC) and total anthocyanin contents (TAC), DPPH, and FRAP assays. BGR at 10–15 days contained the highest TPC (29.72 ± 1.42 mg gallic acid equivalent/g extract) and reducing power (2.22 ± 0.014 mmole FeSO₄/g extract). BGR at 20–25 days contained the highest TAC (0.86 ± 0.096 equivalence of cyanidin-3-glucoside/g extract) and DPPH radical scavenging activity ($IC_{50} = 231.09 \pm 12.99$ µg/mL). Antiproliferative activity of the extracts was evaluated in the human T-lymphocyte (Jurkat), hepatocellular carcinoma (HepG2), colorectal carcinoma (HCT116), melanoma (SK-MEL-2) and noncancerous cells (Vero) by neutral red assay. BGR showed the most selective antiproliferation against Jurkat cells, by inducing apoptosis, and caspase 3/7 activity. BGR at 200 µg/mL from all ages significantly decreased ROS using DCFH-DA and increased endogenous glutathione levels in Jurkat cells compared to the control ($p < 0.05$). The higher antiproliferation of BGR than RD6 was via its antioxidation capacity and attributed to its higher phenolic and anthocyanin contents. BGR sprout is a potential source of biologically active substances good for wellness and health benefits.

Keywords: cancer; antioxidants; antiproliferative activity; black glutinous rice; white glutinous rice; reactive oxygen species

1. Introduction

Cancer is an uncontrollable cell growth developed into abnormal cells that can invade normal body tissue. The major influencing factors include genetic and lifestyle that affect and trigger cancer formation in the body. Cancer formation is the multiple steps involving the transformation of the normal cells into cancer cells (initiated cells), which undergo tumor promotion to become preneoplastic

cells that further progress to neoplastic cells. Carcinogens induced cancer either through molecular targets or cellular effects involving genotoxic and nongenotoxic mechanisms. The genotoxic agent can damage genomic DNA resulting in mutation and clastogenic changes. The nongenotoxic agent alters gene expression and modulates cell growth and cell death. Induction of cancer by nongenotoxic agents can occur in 2 ways; (i) induction of mutations during continual cell division through misrepair results in an initiated preneoplastic cell that may clonally expand to a neoplasm, and (ii) stimulation of the selective clonal growth of already spontaneously initiated cells [1].

In the body, there was a balance between hypoxic stress and oxidative stress called “oxidant homeostasis” [2]. When the level of oxidative stress is high, various antioxidative enzymes and protein systems come to compensate. These antioxidant proteins are such as superoxide dismutase, glutathione peroxidase, glutathione S-transferase, and glutathione [3,4]. Oxidative stress or the overproduction of reactive oxygen species (ROS) plays a pivotal role in all stages of tumor development. The excessive cell proliferation within those carcinogenesis steps also results in the overproduction of ROS, produced from endogenous and exogenous sources. The endogenous sources are such as mitochondria, peroxisomes, cytochrome P450, and inflammatory cells [5]. The exogenous sources are from radiation, pathogens, environmental, and chemical substances [5].

ROS induce several gene mutations at the initiation stage of the cancer process under inhibited antioxidant defense pathways and DNA repair mechanisms. ROS also exerted epigenetic or nongenotoxic effects [6]. The changes in gene expression induced by ROS can be modulated by several signaling pathways. The activation of the transcription factors by ROS is ROS level-dependent. High levels of ROS result in cell death (necrosis or apoptosis). Moderate levels of ROS may induce DNA damage and mutation leading to the formation of an initiated cell (tumor initiation). Low ROS altered the expression of growth factors and proto-oncogenes [7], leading to an increase in cell proliferation of mutated cells (tumor promotion). Low ROS activated transcription factors on signaling pathways such as Nrf2, NF- κ B, AP-1, and HIF-1 α that transcript cell growth regulatory genes.

For many centuries, scientists have conducted studies to prevent the risk of cancer as well as screening chemotherapeutic agents for cancer treatment, leading to the promising bioactive compounds, antioxidants, and nutritional content that is widely found from plant's secondary metabolites [8–10]. In addition, there has been consistently linked between the consumption fruit or plant-based food with evidence of the reduction in cancer due to the chemopreventive effect [11]. Currently, new eating habits and trends in the consumption of nutraceuticals and/or functional foods have increased and gained interest due to their therapeutic potential to help prevent many diseases especially those related to oxidative stress. Their nutritional ingredients and biologically active components have been elucidated for their contribution to protecting human health.

Among the promising plants, rice (*Oryza sativa* L.) is an important nutritional source for more than half-hundred percent around the world and even ninety percent for the Asian population. Rice is an important economic crop especially for the Southeast Asian nations that consume the plant as a staple diet, with various rice cultivars across these countries exhibiting biological activities with potential health benefit on reducing the risk of cancer [12–14]. Previous studies about the advantages of rice—mostly from rice grain—are for health benefits as functional foods, pharmaceuticals, and cosmetics. Rice grain composed of folate, which uses for preventing folate deficiency potentially causing neural tube defects [15], megaloblastic anemia [16], coronary heart diseases [17], Alzheimer's disease [18], and cancer [19]. Rice bran or germ has been reported to comprise high amounts of phenolic compounds, vitamins, minerals, and fibers [20]. The grain of colored rice is composed of carotenoids especially astaxanthin, a red-colored ketocarotenoid with strong antioxidant activity [14].

There are two major types of rice colors—colored rice and white-colored rice—depending on the pericarp, embryo, and caryopsis. These different natural colors of rice indicate not only their cultivated varieties but also phytochemical composition and nutrients [12]. Rice leaves have been reported to contain high chlorophyll content. This plant part photosynthesizes various biologically active compounds and functional substances, which are distributed to the grain and other parts [21,22].

During germination, hydrolytic enzymes in rice grain were activated to decompose macromolecules such as starch and protein for synthesizing new cell constituents, and to alter the micromolecular constituents. Rice grain has been reported to accumulate a significant amount of phenolic and flavonoid compounds such as chalcone, flavones, condensed tannins, ascorbic acid, tocopherol, and anthocyanin, which are antioxidants [23]. Our previous study reported the presence of chlorophylls, flavonoids, phenolics, and anthocyanins in the BGR and RD6 at the same harvest ages [24]. Rice sprouts could, therefore, play a profitable role for health. However, few studies on their biological activity as functional foods have been investigated. In addition, to be used as health benefiting foods, there was an insufficient study on the rice sprouts on their antioxidant as well as antiproliferative capability against cancer cells.

RD6 and BGR are two different glutinous cultivars that are popularly consumed in Northeastern Thailand. RD6 is the white grain, while the black glutinous rice (BGR) is the black grain. The rice sprout can be edible as it is characterized as soft and chewable. Our previous study indicated that the two cultivars consist of several phenolic compounds (i.e., protocatechuic acid, vanillic acid, and rutin) [24], which have been proposed to possess antioxidant properties and could contribute to the anticancer activity. Therefore, our objectives of the study were to determine phenolic compounds, as well as the antioxidant activities of RD6 and BGR, both *in vitro* and in cell models, that could attribute to the anticancer activity. In this study, rice sprouts of these two rice cultivars (RD6 and BGR) were then investigated for their phenolic compounds (total phenolic and total anthocyanin content) that potentially contributed to antioxidant activities (detected by DPPH and FRAP assay), and antiproliferative activity (using neutral red assay) against several cancer cell lines. The most sensitive cell line was further selected for the determination of intracellular oxidative stress (intracellular ROS and GSH) as well as the apoptotic induction (annexin V staining) and caspase 3/7 activity. Our obtained information could be useful for the future development of health food products and/or pharmaceuticals.

2. Materials and Methods

Methanol was bought from RCI Labscan Limited (Bangkok, Thailand). Dulbecco's modified Eagle's medium of high glucose (DMEM), Roswell Park Memorial Institute (RPMI-1640), penicillin/Streptomycin Solution (100x) were from Capricorn Scientific (Ebsdorfergrund, Germany) and 0.25% trypsin-EDTA (1X) was from Gibco (Barcelona, Spain). Fetal bovine serum (FBS) was from Hyclone Laboratories (South Logan, UT, USA). 1,1-Diphenyl-2-picrylhydrazyl (DPPH), 2,4,6-tripyridyl-s-triazine (TPTZ), sodium carbonate, ferric chloride ($\text{FeCl}_3 \cdot 6\text{H}_2\text{O}$) and ferrous sulfate were from Hazardons (Taren Point New South Wales, Australia). DMSO was from Lab-Scan, Analytical Science (Dublin, Ireland). Neutral red (NR) was from Sigma Chemical Co. (St. Louis, MO, USA). Gallic acid was bought from Aldrich Chemistry (St. Louis, MO, USA). The standard anticancer drug Cisplatin was purchased from Boryung (Ansan, Korea) and Docetaxel from Hospira Inc. (Lake Forest, IL, USA). 2',7'-Dichlorodihydrofluorescein diacetate (DCFH-DA) was purchased from Sigma-Aldrich Co. (Jhouzih St., Taipei, Tawan). Glutathione assay kit was purchased from Abnova (Redfern NSW, Australia). Reduced glutathione was purchased from Sisco Research Laboratories Pvt. Ltd. (Anhderi Ghatkopar Link Road, Mumbai, India). The FITC-conjugated annexin V were from BioLegend® (San Diego, CA, USA). Caspase Glo®-3/7 reagent kit was purchased from Promega (Woods Hollow Road, Madison, WI, USA). The other reagents were bought from standard commercial suppliers and are of analytical grade.

2.1. Cell Lines and Cell Culture

Hepatocellular carcinoma (HepG2), human colorectal carcinoma (HCT116), human melanoma (SK-MEL-2), and noncancerous African green monkey kidney (Vero) cell lines were cultured in DMEM. Human immortalized T lymphocyte (Jurkat) cell line was cultured in RPMI-1640. All the cultured cells were growing with 10% fetal bovine serum (FBS), 100 units/mL penicillin, and 100 µg/mL streptomycin.

The cell lines were incubated in an incubator (Thermo Scientific CO₂ Incubators, Waltham, MA, USA) at 37 °C and 5% CO₂ and 95% air.

2.2. Plant Extraction

In this study, the rice sprouts with two different cultivars—black glutinous rice (BGR) and white glutinous rice—(RD6) at different harvest ages—young age (5–7 days), middle age (10–15 days) and old age (20–25 days)—were collected from fertilizer- and pesticide-free farm in Khon Kaen province, Thailand. The fresh rice sprouts were chopped into small pieces and extracted with methanol containing 1% hydrochloric acids (20 g per 1000 mL) and then sonicated for 30 min (Crest Ultrasonics, Bangkok, Thailand). The extract was filtered through filter paper. Then, the solvents were removed by a rotary evaporator (IKA® RV 10 Rotary evaporator, Staufen, Germany) at room temperature and moisture was removed by a freeze drier (Eyela FDU-1200 Freeze dryer, Tokyo, Japan) to obtain the dry residue. Finally, the crude extract was stored under 4 °C in an air-tight container before use.

2.3. Total Phenolic Content (TPC) by Folin–Ciocalteu’s Reagent Method

Total phenolic content (TPC) was determined by Folin–Ciocalteu’s reagent method [25,26]. The concentration of the stock solution of the rice sprout extracts was prepared at 10 mg/mL. Briefly, 15 µL of the extract was mixed with 120 µL of the prepared Folin–Ciocalteu’s reagents and kept in the dark at room temperature for 5 min. Later, 60 g/L sodium carbonate buffer pH 7.5, 120 µL was added into the mixture and kept for another 90 min under the same condition. The absorbance of the blue solution of molybdenum (V) in Folin–Ciocalteu’s reagents was measured at 725 nm with the microplate spectrophotometer (EnSight™, Waltham, MA, USA). Gallic acid was used as a standard antioxidant and as a positive control. The experiments were repeated in four replicates. The standard curve was created from the plot between the absorbances of the blue solutions against the gallic concentrations (final concentrations of 2, 10, 20 and 40 µg/mL). TPC was calculated from a standard curve of gallic acid ($y = 0.643x + 0.0267$, $R^2 = 0.9997$) and expressed as milligrams of gallic acid equivalent per gram of rice sprouts dried extract (mg GAE/g extract).

2.4. Total Anthocyanin Content (TAC)

The anthocyanin content was measured according to the pH differential method [27–29] to determine the colored oxonium formed at pH 1.0 and colorless hemiketal format at pH 4.5. Briefly, the mixture of rice sprout extracts solution in methanol (250 µL) was mixed with either sodium acetate buffer pH 4.5 or potassium chloride buffer pH 1.0 (750 µL) in each well. The extract in methanol was diluted 10 times with two buffers, shaking for 15 min under the dark condition and then centrifuged at 2500× g for 10 min at room temperature. The absorbance of the pigment concentration in each well was measured at 510 and 700 nm at room temperature by using the microplate spectrophotometer (EnSight™). The experiments were performed in triplicates. TAC was calculated following Equation (1). Data were presented as milligrams of cyanidin 3-glucoside equivalents per gram of extract (mg C₃GE/g E).

$$\text{Total anthocyanin content (mg/g)} = [A_{\text{diff}} \times M_w \times DF \times 1000] / [\epsilon] \quad (1)$$

where

A_{510} and A_{700} are the absorbances at 510 nm and 700 nm,

$A_{\text{diff}} = (A_{510} - A_{700})_{\text{pH 1.0}} - (A_{510} - A_{700})_{\text{pH 4.5}}$,

M_w is the molecular weight of cyanidin 3-glucoside (C₃GE), 449.2 g/mol,

DF , a dilution factor (10),

1000, the conversion factor 1000 mg/g,

ϵ is the molar extinction coefficient for 26,900 L mol^{−1} cm^{−1}.

2.5. DPPH Radical Scavenging Assay

The DPPH assay was based on hydrogen atom transfer (HAT) reactions [30,31]. 2,2-Diphenyl-1-picrylhydrazyl or DPPH will generate a stable free radical with an unpaired electron that is delocalized over the entire molecule. Then, the changing of the color from yellow to purple was detected by the UV spectrophotometer. Briefly, various concentrations of the rice sprout extracts dissolved in methanol (between 5 to 1000 µg/mL) and the DPPH reagents were added and mixed in the ratio of 1:1 in the 96 well plates for 30 min in the dark at room temperature. The loss of DPPH radical's absorbance at 517 nm was measured by using a microplate spectrophotometer (EnSight™). Gallic acid, a standard antioxidant was used as a positive control ($y = 21.216x + 2.5088$, $R^2 = 0.9822$). The linear curve was obtained from the plot between gallic acid concentration and DPPH radical scavenging power. The experiments were repeated in five replicates. The DPPH radical scavenging capacity is represented as the percentage of DPPH radical inhibition at 50% (IC_{50}). The percentage of inhibition or %DPPH scavenging effect was calculated following Equation (2).

$$\%DPPH \text{ scavenging effect} = [\text{Abs of control} - \text{Abs of sample}] / [\text{Abs of control}] \times 100 \quad (2)$$

Abs of control = absorbance of control or a reaction mixture in an absence of antioxidant of sample

Abs of sample = absorbance of the reaction mixture in the presence of sample

2.6. Reducing Antioxidant Power Based on FRAP Assay

The FRAP assay describes ferric reducing antioxidant power, the ability of an antioxidant to reduce Fe^{3+} -TPTZ complex to Fe^{2+} -TPTZ [27,32]. Various concentrations of each test compound (e.g., rice sprout extracts or standard antioxidant gallic acid) was mixed with 1 mL DMSO. The FRAP reagent comprised of 300 mM acetate buffer (pH 3.6), 10 mM 2,4,6-tris(2-pyridyl)-s-triazine (TPTZ) solution and 20 mM $FeCl_3 \cdot 6H_2O$ in a 10:1:1 ratio. The reaction mixture was pipetted into each well of a 96-well plate and incubated for 30 min in the dark at room temperature. The absorbance of the colored product (ferrous tripyridyltriazine complex) was measured at 593 nm with the microplate spectrophotometer (EnSight™) against a blank with deionized water. The experiments were repeated in five replicates. The FRAP value was calculated from the standard curve of $FeSO_4$ ($y = 0.5065 - 0.3073x$, $R^2 = 0.9782$) and expressed in mmol Fe^{2+} per gram of extract (mmole Fe^{2+} /g extract). Gallic acid was used as a positive control ($y = 0.3821x + 0.0653$, $R^2 = 0.998$).

2.7. Cytotoxicity Assay by Neutral Red Assay

Neutral red (NR) can diffuse and accumulates intracellularly in the lysosomes of the living cells [32,33]. Cancer cell viability was, therefore, measured using neutral red (NR) assay. Briefly, cells at a density of 5×10^5 cells/mL were seeded with various concentrations of rice sprout extracts for 24 and 48 h. NR solution was added to each well (with a final concentration of 50 µg/mL) and incubated at 37 °C for 2 h. Then, cells were washed twice with 0.01 M PBS and the supernatant was then discarded. Cells were lysed by 0.33% HCl in 100 µL isopropanol. The absorbance of NR dye was detected by the microplate spectrophotometer (EnSight™) at 537 nm with a 650 nm as a reference wavelength. The percentage of cell viability was determined between the absorbance of the treated cells at each concentration of the rice sprout extracts against the absorbance of treated cells with DMSO at the concentration used in the extract concentration. The experiments were repeated in five replicates. The results were expressed as the concentration of the test compound that caused a 50% loss of the cell viability (IC_{50}) when compared to the untreated cells or control. The selectivity index (SI) was also calculated from the ratio of the IC_{50} of normal cells versus the IC_{50} of cancer cells [34].

2.8. Determination of Intracellular Peroxide (H_2O_2) by DCFH-DA Assay

DCFH-DA is non-fluorescent until the acetate group is removed by intracellular esterase and is underwent oxidation in the cell by the intracellular ROS (mainly H_2O_2). ROS oxidizes the free

DCFH-DA to 2',7'-dichlorofluorescein (DCF), and its fluorescent intensity can be measured by flow cytometry [32]. Briefly, DCFH-DA was added to the extract-treated Jurkat cells for 12 h. H_2O_2 was used as a positive control. After the treatment of 12 h of the positive control and samples, all the cells were collected, washed in 0.01 M PBS, and centrifuged at $700\times g$ for 5 min. The supernatant was discarded, and cells were re-suspended in 0.01 M PBS before staining the cells in the dark with 10 μ M DCFH-DA in serum-free medium for 30 min. Once the incubation period was completed, cells were analyzed by flow cytometry (BD FACSCanto II, BD Biosciences, San Jose, CA, USA) within 1 h of staining period. Intracellular ROS was expressed as DCF fluorescence intensity and calculated by BD FACSDiva software. The data were calculated in comparison to the untreated cells and represented as a ratio compared with the untreated cells.

2.9. Determination of the Total Endogenous Glutathione Level

The total endogenous glutathione (GSH) level was analyzed colorimetrically using a glutathione assay kit (Abnova, Taipei, Taiwan). Glutathione (Sisco Research Laboratories Pvt. Ltd., Mumbai, India) with the final concentrations of 125, 250, 500, 750, 1000, 1500 ng/mL was used as a standard in this assay to generate the standard curve to determine the intracellular GSH level ($y = 0.0019x + 0.3842$, $R^2 = 0.9942$). The Jurkat cells were treated with BGR for 12 h. Afterward, cells were lysed with glutathione buffer and incubated on ice for 10 min. Then, the cells were centrifuged at $8000\times g$ for 10 min and the supernatant was collected for the glutathione assay. The reaction mixture of NADPH generation mixture (lyophilized), glutathione reductase, and glutathione reaction buffer was prepared and added to each well and incubated at room temperature. Sample or standard was added following by the substrate (5,5'-dithio-bis-[2-nitrobenzoic acid], DTNB). The total amount of glutathione was detected by the microplate spectrophotometer at a wavelength of 415 nm. The percentage of glutathione levels of treated cells was calculated in comparison to the untreated cells.

2.10. Apoptotic Cell Death Mode by Flow Cytometry

When cells undergo apoptosis, the membrane phospholipid phosphatidylserine (PS) translocates to the outer membranes and binds with annexin V [32]. Briefly, Jurkat cells at 1×10^6 cells/mL were seeded in the plates. After being treated with BGR extract for 24 h, Jurkat cells were washed with 0.01 M PBS centrifuged at $700\times g$ for 5 min. Then, cells were resuspended in annexin V binding buffer and stained with 5 μ L annexin V-FITC for 15 min in the dark at room temperature. Docetaxel (100 μ M), an anticancer drug, was used as a standard apoptosis inducer. Once the incubation period was completed, cells were analyzed by flow cytometry (BD FACSCanto II, BD Biosciences, San Jose, CA, USA) within 1 h after staining. The cells binding with annexin V were classified as apoptotic cells, and the results were displayed as a percentage to the total cell population.

2.11. Caspase 3/7 Activity Assay

Caspase 3/7 assay was done according to manufacturer's instruction in white polystyrene 96 well plates (Promega). The proluminescent caspase-3/7 substrate is cleaved to release aminoluciferin, which will be catalyzed by luciferase to produce the luminescence light. Briefly, 3×10^4 cells/mL of Jurkat cells were seeded in the plates and were treated with BGR extract for 24 h. Docetaxel (10 μ M) was used as a positive control. After completing the treatment, caspase Glo[®]-3/7 reagents were added into the cells and equilibrated for 1 h at room temperature. Luminescence mode was measured by using a microplate spectrophotometer. The percentage of caspase 3/7 activity was calculated in comparison to the untreated cells.

2.12. Statistical Analysis

Experimental results are presented as mean \pm standard deviation (SD). Statistical analyses between groups were performed by using one-way ANOVA followed by Tukey multiple comparison tests.

A significant difference was set at $p < 0.05$. Regression and partial correlation analysis were performed using SPSS 25 (SPSS Inc, Chicago, IL, USA).

3. Results and Discussion

3.1. Extraction Yield of Rice Sprouts

Results of the extraction yield of BGR and RD6 at different ages were shown in Table 1. The lower %yields of plant extract were found in BGR groups than in RD6 groups. RD6 at 20–25 days had the highest %yields per fresh weight, whereas BGR at 5–7 days had the lowest %yields. The rank order from high to low extraction yield were RD6 20–25 (63.50%), RD6 5–7 (60.12%), RD6 10–15 (25.97%), BGR 10–15 (13.30%), BGR 20–25 (13.25%) and BGR 5–7 (8.69%), respectively.

Table 1. Extraction yield of rice sprouts at different ages and heights.

Age (Day), and Height of Rice Sprouts (cm)		% Yields (w/w Fresh Weight)
BGR	5–7 days, 5–7 cm	8.69% ⁶
	10–15 days, 10–12 cm	13.30% ⁴
	20–25 days, 15–17 cm	13.25% ⁵
RD6	5–7 days, 5–7 cm	60.12% ²
	10–15 days, 10–12 cm	25.97% ³
	20–25 days, 15–17 cm	63.50% ¹

Superscript numbers from 1 to 6 assigned for high¹ to low⁶ % extraction yield.

3.2. In Vitro Antioxidant Capability

3.2.1. Determination of Total Phenolic Content by Folin–Ciocalteu’s Reagent Method

The methanolic extract of BGR at 10–15 days contained 29.72 ± 1.42 mg GAE/g extract, which is higher than BGR 20–25 (23.44 ± 1.04 mg GAE/g extract), BGR 5–7 (6.30 ± 0.70 mg GAE/g extract), RD6 10–15 (4.07 ± 0.17 mg GAE/g extract), RD6 20–25 (2.59 ± 0.29 mg GAE/g extract) and RD6 5–7 days (1.19 ± 0.09 mg GAE/g extract), respectively (Figure 1a).

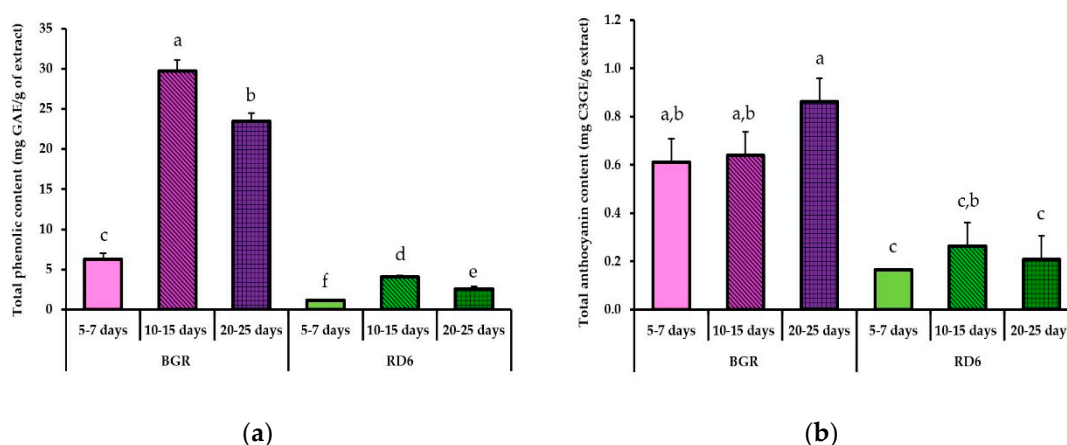


Figure 1. (a) Total phenolic content (TPC) of black glutinous rice (BGR) and RD6 according to Folin–Ciocalteu’s reagent methods. (b) Total monomeric anthocyanin content (TAC) of BGR and RD6 according to the pH differential methods. Results expressed as mean \pm SD with four replicates for TPC and three replicates for TAC. The letters indicate statistically significant ($p < 0.05$) among samples.

3.2.2. Determination of Total Anthocyanin Content

In general, BGR contained significantly higher total anthocyanin content (TAC) than RD6 (Figure 1b). TAC in BGR was positively correlated to the increasing age. BGR at 20–25 days exhibited the highest

TAC content of 0.86 ± 0.096 mg C₃GE/g extract followed by BGR at 10–15 days (0.64 ± 0.096 mg C₃GE/g extract), BGR at 5–7 days (0.61 ± 0.096 mg C₃GE/g extract), RD6 at 10–15 days (0.26 ± 0.096 mg C₃GE/g extract), RD6 at 20–25 days (0.21 ± 0.096 mg C₃GE/g extract), RD6 at 5–7 days ($0.17 \pm 6.7 \times 10^{-16}$ mg C₃GE/g extract), respectively.

3.2.3. Determination of DPPH Radical Scavenging Effect

DPPH is decolorized by antioxidant or radical scavenging agents [16]. Results are expressed as half maximal inhibitory concentration value (IC₅₀) (μg/mL) ± SD (Table 2). BGR showed significant scavenging activities than RD6 ($p < 0.05$), and lesser than gallic acid. BGR at 20–25 days and 10–15 days showed higher scavenging activities, with the lowest IC₅₀ value of 231.1 ± 12.9 and 238.8 ± 10.4 μg/mL than the age 5–7 days (271.2 ± 13.1 μg/mL).

Table 2. 1,1-Diphenyl-2-picrylhydrazyl (DPPH) radical scavenging activity of rice sprout extracts. The half-maximal inhibitory concentration (IC₅₀) is a measurement of the effectiveness of the extract in inhibiting DPPH radical.

Test Compounds	Ages (days)	IC ₅₀ (μg/mL) ± SD
BGR	5–7	271.2 ± 13.1^a
	10–15	238.8 ± 10.4^a
	20–25	231.1 ± 12.9^a
RD6	5–7	571.7 ± 17.4^b
	10–15	575.8 ± 38.2^b
	20–25	636.7 ± 34.6^c
Gallic acid	-	2.24 ± 0.03

Data are expressed as mean ± SD from five replicates. Different letters indicate a significant difference between test compounds ($p < 0.05$).

3.2.4. Determination of Ferric Reducing Antioxidant Power

FRAP values indicated that the BGR possessed the greater ferric reducing power than RD6. The reducing power of BGR at each age increases in a concentration-dependent manner. BGR at 10–15 days and 20–25 days showed higher reducing ability (2.22 ± 0.014 and 1.58 ± 0.0302 mmoles of FRAP power per weight in gram unit of extracts at 1000 μg/mL, respectively) (Table 3) than other harvest ages within the same and different cultivars.

Table 3. Ferric reducing power of rice sprout extracts. Data are expressed as mean ± SD of absorbance ferric-to-ferrous reduction capacity of BGR and RD6 from five replicates ($p < 0.05$).

Rice Cultivars	Ages (days)	FRAP Power (mmole) Per Weight in Gram of Extract		
		100 μg/mL	200 μg/mL	1000 μg/mL
BGR	5–7	0.79 ± 0.0051^{cC}	0.84 ± 0.0068^{cB}	1.28 ± 0.015^{cA}
	10–15	1.37 ± 0.017^{aC}	1.86 ± 0.069^{aB}	2.22 ± 0.014^{aA}
	20–25	1.28 ± 0.011^{bB}	1.61 ± 0.115^{bA}	1.58 ± 0.0302^{bA}
RD6	5–7	0.73 ± 0.004^{eC}	0.76 ± 0.0049^{dB}	0.93 ± 0.0083^{fA}
	10–15	0.77 ± 0.016^{dC}	0.85 ± 0.061^{cB}	1.21 ± 0.016^{dA}
	20–25	0.73 ± 0.019^{eB}	0.76 ± 0.018^{dB}	1.03 ± 0.019^{eA}

Data were presented in mean ± SD ($n = 5$). Different lower-case letters indicate a significant difference in columns (same concentration at different ages) and different capital letters indicate a significant difference in a row (different concentrations at the same ages) ($p < 0.05$).

3.3. Determination of Cell Viability in Various Cancer and Noncancer Cell Lines

The cell viability assay of rice sprout extracts at 24 and 48 h was performed using a neutral red assay in various cell lines including HepG2, HCT116, SK-MEL-2, and Jurkat, which have never

been previously reported. Cisplatin, a standard anticancer drug, was used as a positive control [35]. Results showed that at 24 h cisplatin showed strong to low antiproliferation on HCTT116, SK-MEL-2, Jurkat, HepG2, and Vero, respectively (Table 4).

Table 4. The effect of rice sprout extracts on cell viability of various cancerous (Jurkat, HepG2, HCT116, and SK-MEL-2) cell lines and noncancerous (Vero) cell line at 24 and 48 h. Data expressed as mean \pm SD of half-maximal inhibitory concentration (IC_{50}) from five replicates.

Time	Compounds	Ages (Days)	IC_{50} (μ g/mL) \pm SD (Selectivity Index)				
			Jurkat	HepG2	HCT116	SK-MEL-2	Vero
24 h	Cisplatin		61.8 \pm 1.3 ^a	65.1 \pm 0.6 ^a	25.8 \pm 0.5 ^a	27.7 \pm 0.5 ^a	121.5 \pm 1.6 ^a
		5–7	206.2 \pm 15.1 ^{aA} (4.8)	Inactive ^{bC}	806.2 \pm 16.0 ^{cB} (1.2)	Inactive ^{bC}	Inactive ^{bC}
		10–15	261.9 \pm 6.6 ^{bA} (3.8)	Inactive ^{bC}	513.4 \pm 18.3 ^{bB} (1.9)	Inactive ^{bC}	Inactive ^{bC}
	BGR	20–25	438.6 \pm 11.6 ^{dB} (2.3)	Inactive ^{bC}	426.4 \pm 6.1 ^{aA} (2.3)	Inactive ^{bC}	Inactive ^{bC}
		5–7	Inactive ^{eA}	Inactive ^{bA}	Inactive ^{dA}	Inactive ^{bA}	Inactive ^{bA}
		10–15	310.2 \pm 28.0 ^{cA} (3.2)	Inactive ^{bB}	Inactive ^{dB}	Inactive ^{bB}	Inactive ^{bB}
		20–25	Inactive ^{eA}	Inactive ^{bA}	Inactive ^{dA}	Inactive ^{bA}	Inactive ^{bA}
	RD6	5–7	67.62 \pm 6.8 ^{aA} (14.8)	323.7 \pm 18.5 ^{aB} (3.1)	439.4 \pm 22.7 ^{cC} (2.3)	Inactive ^{dD}	Inactive ^{aD}
		10–15	166.7 \pm 13.2 ^{bA} (6.0)	Inactive ^{bC}	391.0 \pm 54.3 ^{ab,B} (2.6)	Inactive ^{dC}	Inactive ^{aC}
48 h	BGR	20–25	136.4 \pm 4.9 ^{ab,A} (7.3)	326.5 \pm 19.0 ^{aB} (3.1)	379.0 \pm 11.0 ^{aB} (2.6)	Inactive ^{dD}	Inactive ^{aD}
		5–7	Inactive ^{dA}	Inactive ^{bA}	Inactive ^{dA}	Inactive ^{aA}	Inactive ^{aA}
		10–15	508.2 \pm 20.8 ^{cA} (2.0)	Inactive ^{bB}	Inactive ^{dB}	677.8 \pm 35.7 ^{bA} (1.5)	Inactive ^{aB}
	RD6	20–25	Inactive ^{dA}	Inactive ^{bA}	Inactive ^{dA}	Inactive ^{aA}	Inactive ^{aA}

The cytotoxicity percentage were presented as mean \pm SD ($n = 5$). Inactive is indicated as $> 50\%$ cytotoxicity when treated with the samples at the maximum concentration (1000 μ g/mL). Different lower-case letters indicate a significant difference of test samples in a row (different cell lines, same treatment) and different capital letters indicate a significant difference in column (same cell line, different treatments) ($p < 0.05$).

At 24 h, Jurkat was the most sensitive cell line responding to BGR at all ages and RD6 at 10–15 days as indicated by the lowest IC_{50} value. BGR at age 5–7, 10–15 and 20–25 days decreased cell viability of Jurkat with the respective IC_{50} values of 206.2 \pm 15.1, 261.9 \pm 6.6, 438.6 \pm 11.6 μ g/mL when compared to control ($p < 0.0001$). RD6 at 10–15 days reduced the cell viability of Jurkat cells (IC_{50} value of 310.2 \pm 28.0 μ g/mL) while the other ages of RD6 were inactive to Jurkat cells. HCT116 was the second cell line upon which BGR exerted a low reduction of cell viability. BGR and RD6 extracts were inactive in HepG2, SK-MEL-2, and Vero cells at 24 h (Table 4).

At 48 h, Jurkat was the most sensitive cell line responding to BGR following by HCT116 and HepG2. BGR showed greater inhibition of cell viability at 48 h than those of 24 h. BGR at 5–7, 10–15 and 20–25 days inhibited cell viability of Jurkat cells with the respective IC_{50} values of 67.62 \pm 6.8, 166.7 \pm 13.2, 136.4 \pm 4.9 μ g/mL compared to the control ($p < 0.05$). HCT116 and HepG2 displayed low sensitivity to BGR ($p < 0.05$). Both BGR and RD6 were inactive in SK-MEL-2 and Vero at 48 h (Table 4). Notably, BGR and RD6 were inactive to Vero cells at both 24 and 48 h.

The selectivity index (SI) indicates selective inhibition of cancer cell viability of the tested compound in comparison to the noncancerous cells [34,36]. The SI values of BGR extracts on Jurkat cells were increased in a time-dependent manner. Moreover, HepG2 cells become more sensitive to some BGR extract with increasing SI values at 48 h when compared to 24 h. RD6 at only 10–15 days highly selective inhibited cell viability of Jurkat cells at 24 h (SI = 3.2) (Table 4) and this extract did not show higher SI value at the longer time point (48 h) in Jurkat cells but gain slight selectivity (SI = 1.5) in SK-MEL-2 cells at 48 h.

3.4. Determination of Intracellular Hydrogen Peroxide Level in Jurkat Cells

Antioxidant activity of BGR in the Jurkat cells was determined whether it was contributed to its anticancer activity. The intracellular ROS level was presented as a bar graph in Figure 2a. Results showed that at 12 h H_2O_2 (0.1 $\mu\text{g/mL}$) significantly increased ROS level ($121.17 \pm 7.36\%$) in Jurkat cells compared to the untreated cells ($100 \pm 3.29\%$) ($p < 0.05$). BGR at $0.5 \times \text{IC}_{50}$ (100 $\mu\text{g/mL}$) and $1 \times \text{IC}_{50}$ (200 $\mu\text{g/mL}$) concentrations obtained from the cell viability assay were determined for their antioxidant activity in the Jurkat cells. BGR at 5–7, 10–15 and 20–25 days (100 $\mu\text{g/mL}$) decreased ROS level in Jurkat cells to $67.03 \pm 1.70\%$, $51.38 \pm 4.51\%$, $45.93 \pm 1.79\%$, respectively. A greater reduction in ROS was found after BGR treatment at 200 $\mu\text{g/mL}$ at age of 5–7, 10–15 and 20–25 days to $39.13 \pm 3.36\%$, $28.66 \pm 2.17\%$, $22.76 \pm 1.37\%$, respectively. Different harvest ages of BGR showed different cellular antioxidant ability with concentration-and age-dependent manner ($p < 0.05$) (Figure 2a). BGR at $1 \times \text{IC}_{50}$ concentration at the age of 20–25 days displayed the most effective antioxidant activity.

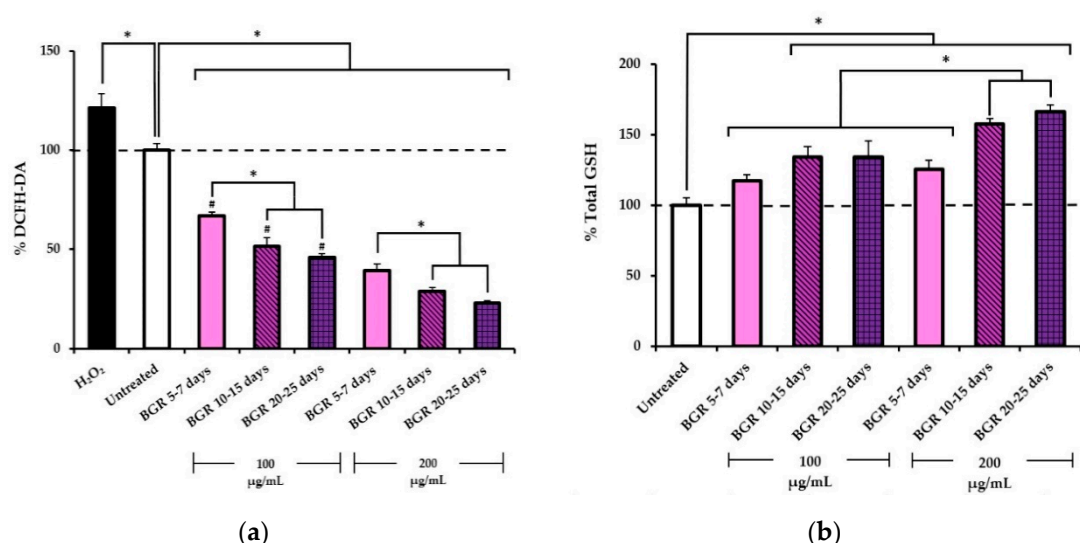


Figure 2. (a) Flow cytometry analysis of intracellular ROS (H_2O_2) by DCFH-DA assay. H_2O_2 (0.1 $\mu\text{g/mL}$) was used as a positive control. Data are expressed as mean \pm SD of four replicates. (b) Total endogenous glutathione (GSH) level in the Jurkat cells treated with BGR. Data are expressed as mean \pm SD of triplicates. (*) Value is significantly different ($p < 0.05$). (#) $p < 0.05$ when compared the same extract at different concentrations.

3.5. Determination of Endogenous Glutathione Level in Jurkat Cells

The BGR at 100 and 200 $\mu\text{g/mL}$ significantly increased the endogenous glutathione level ($p < 0.05$) compared to the untreated group ($100.00 \pm 5.72\%$) (Figure 2b). A higher GSH level were found in Jurkat cells treated with 200 $\mu\text{g/mL}$ BGR aged 5–7, 10–15 and 20–25 days ($125.80 \pm 6.54\%$, $157.65 \pm 4.27\%$ and $166.54 \pm 5.04\%$, respectively) than cells treated with 100 $\mu\text{g/mL}$ ($117.31 \pm 4.32\%$, $134.26 \pm 7.54\%$ and $134.17 \pm 11.77\%$, respectively). The GSH level was increased in the treated cells depending on the concentration and the harvest age of BGR.

3.6. Apoptosis Induction Effect

3.6.1. Apoptosis Induction According to Flow Cytometric Analysis

Apoptosis is the programmed cell death that is a hallmark of the anticancer action of the tested compound [32,37]. BGR at two different concentrations according to the cell viability assay ($0.5 \times \text{IC}_{50}$ or 100 $\mu\text{g/mL}$ and $1 \times \text{IC}_{50}$ or 200 $\mu\text{g/mL}$) were used in this assay. At 100 $\mu\text{g/mL}$, BGR at 3 different ages (5–7, 10–15 and 20–25 days) induced apoptosis ($12.8 \pm 1.4\%$, $11.3 \pm 2.3\%$ and $17.7 \pm 6.1\%$, respectively) compared to the untreated cells ($15.9 \pm 1.2\%$) (Figure 3a). At higher concentration (200 $\mu\text{g/mL}$),

BGR at 10–15 and 20–15 days significantly caused apoptotic cell death for 30.5 ± 3.9 and $31.2 \pm 4.9\%$, respectively (Figure 3a). Increasing concentration of BGR increased apoptotic cell death. The standard anticancer drug, docetaxel at $100 \mu\text{M}$ was used as a positive control and was found to strongly induce apoptosis ($56.5 \pm 3.1\%$) in Jurkat cells. Our results suggested that BGR at different harvest ages induced Jurkat cells to die via apoptosis.

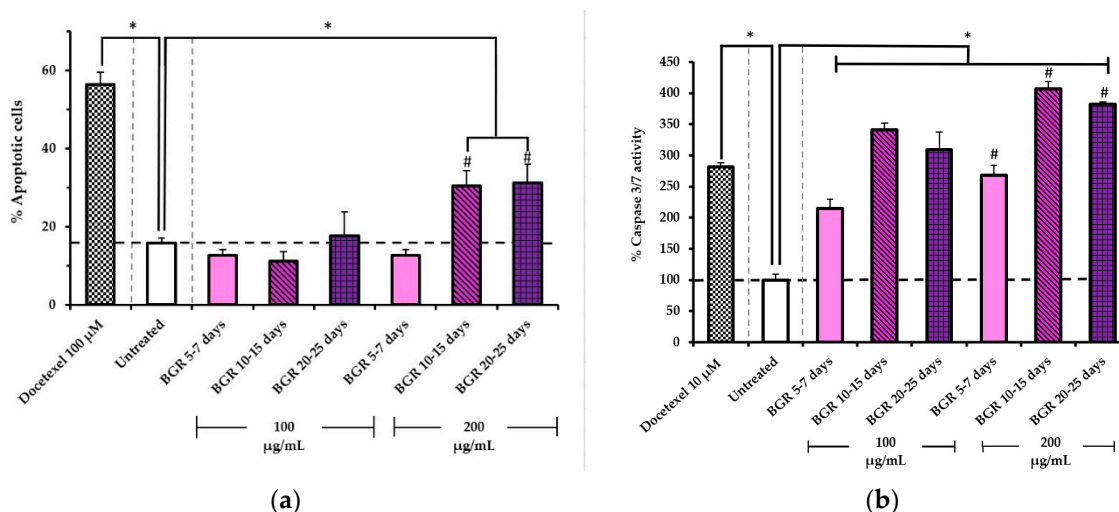


Figure 3. (a). % Apoptotic cell of Jurkat cells after 24 h incubation with rice sprouts (BGR) at different harvest ages using annexin V staining and flow cytometry analysis. Docetaxel $100 \mu\text{M}$ was used as a positive control. (b). Caspase 3/7 activity in Jurkat cells treated with 100 and $200 \mu\text{g/mL}$ of BGR at different harvest ages at 24 h. Docetaxel at $10 \mu\text{M}$ was used as a positive control. Data are expressed as the mean \pm SD of four replicates. (*) Value is significantly different ($p < 0.05$) from untreated group (100%). (#) $p < 0.05$ when compared in the same extract at different concentrations.

3.6.2. Caspase 3/7 Activity Assay

To confirm the apoptosis-inducing effect of BGR, the caspase 3/7 activity was determined as the enzymes are activated during apoptosis. BGR at both 100 and $200 \mu\text{g/mL}$ at 5–7, 10–15 and 20–15 days induced apoptosis at 24 h that indicated by the significantly increased activity of caspase 3/7 in Jurkat cells in comparison with the untreated cells or the control ($100.00 \pm 9.26\%$) ($p < 0.05$) (Figure 3b). The standard anticancer drug docetaxel at $10 \mu\text{M}$ was used in this study as it is clinically used in leukemia [38–40]. Docetaxel strongly increased the caspase 3/7 activity at $281.56 \pm 7.26\%$ compared to the control. A higher caspase 3/7 activity was found when Jurkat cells were treated with $200 \mu\text{g/mL}$ BGR than those with $100 \mu\text{g/mL}$.

At $100 \mu\text{g/mL}$, BGR at 5–7, 10–15 and 20–25 days increased caspase 3/7 activity to $215.36 \pm 14.54\%$, $340.85 \pm 11.29\%$, $308.98 \pm 28.94\%$, respectively compared to the untreated cells. And at $200 \mu\text{g/mL}$, BGR at 5–7, 10–15 and 20–25 days increased caspase 3/7 activity to $267.79 \pm 16.91\%$, $407.13 \pm 11.63\%$, $382.57 \pm 3.40\%$, respectively compared to the untreated cells (Figure 3b). BGR induced apoptosis via increasing caspase 3/7 activity in a concentration-dependent manner. Notably, $200 \mu\text{g/mL}$ of BGR at 10–15 days increased caspase 3/7 activity at a 4 times higher than the control.

4. Discussion

Sprouts of black (cv. BGR) and white (cv. RD6) glutinous rice with the different harvest ages (5–7, 10–15, and 20–25 days or young, middle and old age) showed different degree of antioxidant capacity. The *in vitro* antioxidant capacity of BGR is higher than RD6 based on TPC, TAC, DPPH, and FRAP assays. The hydroxyl group of phenolic compounds and anthocyanin has been reportedly responsible for antioxidant activity [41–44]. DPPH yields a stable free radical of unpaired electron delocalized over the entire molecule. The scavenging activity of BGR and RD6 resulted in a decrease in DPPH radical

absorption proportional to the concentration of radicals that were scavenged. The lowest IC₅₀ from DPPH assay of middle and old age of BGR showed the greatest scavenging activity among harvest ages and cultivars ($p < 0.05$). Moreover, the single-electron transfer mechanism based on the ferric ion reducing capability of BGR and RD6 was evident. Interestingly, BGR at middle and old age exhibited greater ferric reducing antioxidant power (FRAP) than RD6.

A previous study reported on the antioxidant activity of the rice grass juices of various rice cultivars based on DPPH and FRAP assays [27]. The colored grass juice can prevent oxidative damage of supercoiled pBR322 DNA in a dose-dependent DNA protective effect. Their results showed that the colored rice (cv. Kum) possessed higher TPC than the white rice cultivar (cv. RD6). Moreover, TAC was also high in colored rice grass juices. The colored grass juice of Kum Doisaket (cv. C-KDS) contained TAC higher than the other colored rice. These results are in agreement with our study regarding the higher TPC, DPPH scavenging activity, and ferric reducing antioxidant power of colored rice (BGR) than that of white-colored rice (RD6).

Different harvest ages of BGR exhibited cytotoxic effects on Jurkat and HCT116 at 24 h and at 48 h and on HepG2 cells at 48 h. BGR at 5–7 days and 10–15 days showed high selective cytotoxic (with SI > 3) against Jurkat cells at 24 h and 48 h ($p < 0.05$) when compared to RD6. At 48 h, BGR at 5–7 days and 20–25 days displayed high selectivity (SI ≥ 3) against HepG2. Notably, the Vero cells were not sensitive to any compounds, indicating the safety of BGR and RD6 in the noncancerous cells. Cytotoxicity results of BGR are well correlated with the *in vitro* antioxidant activity, which is higher than RD6. A further anticancer effect of BGR extract on the Jurkat cells was directly examined.

In the present study, the causes of high cytotoxic effects of BGR in Jurkat cells were investigated vis-à-vis intracellular ROS (e.g., H₂O₂) and endogenous glutathione levels. BGR at middle and old age effectively decreased the ROS level in Jurkat cells at 12 h in a concentration-dependent manner. Moreover, a decrease in cellular ROS level corresponded with an increase in endogenous GSH in cells treated with BGR at 12 h. BGR increased GSH to circumvent oxidative damage caused by ROS in Jurkat cells. During a high level of intracellular ROS such as H₂O₂, GSH cleaves H₂O₂ via GSH reductase to convert ROS to H₂O [1,45]. The middle and old age of BGR demonstrated the greatest antioxidant activity in Jurkat cells as a ROS reducer and GSH activator.

The excessive production of ROS in normal cells leads to the initiation of DNA damage and carcinogenesis [1,5,46,47]. Many plants have been reported to possess the antioxidant properties to decrease the ROS level in cancer cells [48–50]. Low ROS level plays an important part in cellular signaling, cell proliferation, and apoptosis [1,51]. Moreover, cells have mechanisms to repair damaged DNA. However, if the damaged DNA cannot be repaired, cells will undergo apoptotic cell death. DNA damage-induced apoptosis is a cellular defense mechanism to eliminate genetically damaged cells [52,53]. Apoptosis induction is, therefore, an endpoint for screening anticancer action [54,55].

Our study found that BGR induced apoptosis in Jurkat cells at 24 h. During apoptosis, DNA is condensed and fragmented, and there is an externalization of phosphatidylserine to the outer side of the cell membrane of apoptotic cells. Later, phagocyte molecules involve in recognition and remove unrepairable apoptotic cells without triggering inflammation [55]. The flipping of phosphatidylserine can specifically bind with annexin V that can be detected by flow cytometry to indicate the early stage of apoptosis [55]. The cytotoxic effect of BGR occurred via apoptosis as the Jurkat treated cells were stained with annexin V. Moreover, caspase 3/7, that is the downstream effector caspases in the caspase cascade pathway [56], was increased in the BGR-treated Jurkat cells. Our results indicated that BGR induced an early stage of apoptosis detected by cells stained with annexin v measuring by flow cytometry and induced Jurkat cells to die via apoptotic death mode as observed from the increasing of caspase 3/7 activity. A previous study also reported that the fermented mixture of brown rice and rice bran induced apoptosis in human acute lymphoblastic leukemia cells [57], which is in agreement with our study. Several studies reported the contribution of plant phenolic content to antioxidant, cytotoxicity, and apoptosis in cancer cell lines [58,59] as well as anthocyanin, one of the flavonoid

groups, for its cancer prevention activity [60,61]. Hence, the phenolic content and anthocyanin content of BGR may contribute to its antioxidant, cytotoxicity, and apoptosis in the Jurkat cells.

It should be noted that rice sprout is a young green leaf where the second metabolites or active compounds are synthesized after photosynthesis. The difference in the types and contents of compounds in the same plant found between studies could be affected by several factors such as different harvest time, age, parts, growing condition, and the type of solvent used for the extraction. The previous study extracted the rice sprout (20 g) with 1% hydrochloric acid in methanol (100 mL) twice each by sonication for 30 min [24]. Our study extracted the rice sprout (20 g) with 1% hydrochloric acid in methanol 1000 mL and sonicated for 30 min.

A previous study of BGR and RD6 at the same harvest ages reported the existence of important phytochemicals, including total chlorophyll content (TCC), total flavonoid content (TFC), total phenolic content (TPC), total anthocyanin content (TAC), and the proximate composition (i.e., ash, moisture, fat, protein, carbohydrate, energy, and dietary fiber content) [24]. Moreover, protocatechuic acid, vanillic acid, and rutin were quantified in a different amount in BGR and RD6 [24]. The BGR and RD6 rice sprout used in the previous and the present study were at the same harvest age and grown under the same condition but extracted with a slightly different method. Moreover, the extract from BGR and RD6 could comprise of other phytoconstituents besides these identified compounds. The content of protocatechuic acid, vanillic acid, and rutin was not re-analyzed in the present study. Instead, the marker compounds—TPC and TAC—were quantified in the extract, as they reportedly attribute to antioxidation, antiproliferation, and apoptosis induction effects in other plants of other studies.

In the previous study [24], BGR at 10–15 days contained the highest TCC (40.8 ± 0.8 mg/g extract), and BGR at 5–7 days contained the highest TAC (22.13 ± 0.002 mg cyanidin 3-glucoside (C_3GE)/g extract), whereas RD6 at 5–7 days comprised the highest TFC and TPC (34.2 ± 3.4 mg quercetin equivalent (QE)/g extract, and 44.8 ± 1.6 mg gallic acid equivalent (GAE)/g extract, respectively). Moreover, the proximate compositions with 100 g fresh weight of the rice sprouts from both BGR and RD6 had a total ash 2.86 to 5.78 g, moisture 64.72 to 79.11 g, fat 0.32 to 1.2 g, protein 3.38 to 5.99 g, carbohydrate 12.22 to 24.54 g, and energy 73.44 to 124.0 Kcal. The dietary fiber of BGR at 10–15 days was 1.4 times higher than that of RD6 (16.92, and 11.98 and g/100 g fresh weight, respectively). The higher TPC was observed in the BGR group at 10–15 days in the previous study (31.9 ± 1.1 mg GAE/g extract) than our result of BGR at the same age (29.72 ± 1.42 mg GAE/g extract). In the previous study, the highest TAC was found in BGR at 5–7 days (22.13 ± 0.002 mg C_3GE /g extract). The highest TAC in our present study was found in BGR at 20–25 days only at 0.86 ± 0.096 mg C_3GE /g extract. The TAC in the present study was less than the previous reported result, which might be due to the different extraction methods.

Interestingly, the total bioactive compounds (TAC and TPC) were well correlated to the increasing of BGR ages ($r > 0.6$ with $p < 0.05$), not RD6 ($r < 0.6$ with $p > 0.05$) (Supplementary Materials, Figure S1 and Figure S2). In contrast, there is no correlation between BGR ages and FRAP ($r = 0.314$ with $p > 0.05$) (Supplementary Materials, Figure S1), whereas RD6 age was correlated to only DPPH ($r = 0.606$ with $p < 0.05$) (Supplementary Materials, Figure S2). TAC displayed no correlation with both DPPH and FRAP but TPC from both BGR and RD6 demonstrated well correlation to FRAP ($r = 0.891$ and $= 0.986$, respectively with $p < 0.05$). The result implied that TPC was the major bioactive constituents that contribute to the direct antioxidative activity of BGR and RD6 *in vitro*. Moreover, BGR displayed the time-dependent cytotoxic activity to the sensitive cell lines (Jurkat and HCT116), whereas RD6 possessed less potency to the treated cell lines, except SK-MEL-2, with no time-dependent cytotoxicity. The correlation data indicated that Jurkat cell viability increased as BGR ages increased from young to old age at 24h ($r = 0.952$ with $p < 0.05$) and at 48h ($r = 0.586$ with $p < 0.05$), while HCT116 cell viability decreased with ages ($r = -0.951$ with $p < 0.05$) and at 48h ($r = -0.609$ with $p < 0.05$) (Supplementary Materials, Figure S3).

Since Jurkat was the most sensitive cell line to BGR, the further correlation analysis between BGR ages and intracellular biological activities (ROS reduction, increase in GSH, caspase activity,

and apoptosis induction) had been performed. BGR decreased intracellular ROS ($r = -0.943$ with $p < 0.05$) and increased intracellular GSH ($r = 0.922$ with $p < 0.05$), with increasing ages. The good correlation between the reduction of intracellular ROS and an increase in GSH was observed ($r = -0.891$ with $p < 0.05$). Caspase 3/7 activity ($r = 0.782$ with $p < 0.005$) and the percentage of apoptotic cells ($r = 0.824$ with $p < 0.05$) were increased with the increasing ages (Supplementary Materials, Figure S1). The antioxidant capacity in the cell-based assays (from DCFH-DA and GSH assays) was directly correlated with TPC ($r > 0.6$; $p < 0.05$), while cytotoxicity was inversely correlated with TPC ($r < -0.6$; $p < 0.05$). Results implied that TPC predominantly contributed to antioxidant activities *in vitro* and indirectly enhanced intracellular GSH, resulting in a lower intracellular ROS. In addition, TPC could trigger cancer cells to undergo apoptosis as indicated by the increase in caspase 3/7 activity.

In the present study, the phenolic and anthocyanin compounds play a pivotal role for a higher antioxidant capacity as well as apoptosis induction in the Jurkat cells via the activation of the caspase family and other key cellular components of the colored rice (BGR) than those of the white-colored rice (RD6). To compare, BGR exerted greater cytotoxic effect, antioxidant effects, and induce cell death via apoptosis than RD6. The colored rice BRG could be the preferable sprouts for developing as a functional food in the future.

5. Conclusions

Our findings suggested that BGR extract could probably induce the apoptotic death of human acute lymphoblastic leukemia cells, mainly through the death receptor-mediated pathway and through antioxidative effects, proposing the possibility that BGR was a potential functional food and might be beneficial to patients with hematological cancer. The obtained information illustrated the easy-material-accessibility, economic value, environmental benefits from an edible rice sprout. Further study is required to confirm the clinical effectiveness and safe consumption.

Supplementary Materials: The following are available online at <http://www.mdpi.com/2076-3417/10/20/7051/s1>, **Figure S1:** Correlation coefficient (r) of BGR group at different harvest ages with antioxidant capacity (TPC, TAC, DPPH, FRAP, DCFH-DA and GSH), and anticancer effect (cytotoxicity, apoptosis, and caspase activity). If the r value is close to +1 or -1, it will indicate a strong positively relationship or inverse relationship, respectively. If r is near to 0, it will indicate weak or no relationship. * Correlation is significant at $p < 0.05$, **Figure S2:** Correlation coefficient (r) of antioxidant capacity (TPC, TAC, DPPH, and FRAP) of RD6 at different harvest ages. If the value is close to +1 or -1, it will indicate a strong positively relationship or inverse relationship, respectively. If r is near to 0, it will indicate weak or no relationship. *Correlation is significant at $p < 0.05$, **Figure S3:** Correlation coefficient of cytotoxicity between Jurkat and HCT116 after BGR treatment (A) at 24 h and (B) at 48 h. If the value is close to +1 or -1, it will indicate a strong positively relationship or inverse relationship, respectively. If r is near to 0, it will indicate weak or no relationship. *Correlation is significant at $p < 0.05$.

Author Contributions: Conceptualization, N.W.; methodology, V.S., P.P. and N.W.; validation, V.S., P.P., and N.W.; formal analysis, V.S., and N.W.; investigation, V.S., P.P., and N.W.; resources, J.W., W.T., N.W.; data curation, V.S., K.S., B.S. and N.W.; writing—original draft preparation, V.S., P.P. and N.W.; writing—review and editing, V.S., and N.W.; visualization, V.S., and N.W.; supervision, K.S., B.S. and N.W.; project administration, N.W.; funding acquisition, N.W. All authors have read and agreed to the published version of the manuscript.

Funding: V.S. was scholarly supported by (a) the Faculty of Pharmaceutical Sciences, and (b) the Graduate School, Khon Kaen University, Thailand. P.P. has received a scholarship under the Post-Doctoral Training Program from Khon Kaen University (Grant no. PD-2563-09).

Acknowledgments: V.S. was supported for his Master's degree by the Royal Scholarship under Her Royal Highness Princess Maha Chakri Sirindhorn Education Project to the Kingdom of Cambodia. The authors thank (a) Faculty of Pharmaceutical Science, Khon Kaen University and the Human High Performance and Health Promotion Research Institute, Khon Kaen University, Thailand for the facilities and financial support.

Conflicts of Interest: The authors declare no conflict of interest.

References

1. Klaunig, J.E.; Wang, Z. Oxidative stress in carcinogenesis. *Curr. Opin. Toxicol.* **2018**, *7*, 116–121. [CrossRef]
2. Zhang, J.; Wang, X.; Vikash, V.; Ye, Q.; Wu, D.; Liu, Y.; Dong, W. ROS and ROS-mediated cellular signaling. *Oxi. Med. Cell. Longev.* **2016**, *2016*, 1–18. [CrossRef] [PubMed]

3. Kanwal, R.; Pandey, M.; Bhaskaran, N.; MacLennan, G.T.; Fu, P.; Ponsky, L.E.; Gupta, S. Protection against oxidative DNA damage and stress in human prostate by glutathione S-transferase P1: GSTP1. *Mol. Carcinog.* **2014**, *53*, 8–18. [[CrossRef](#)] [[PubMed](#)]
4. Mari, M.; Morales, A.; Colell, A.; García-Ruiz, C.; Fernández-Checa, J.C. Mitochondrial glutathione, a key survival antioxidant. *Antioxid. Redox Signal.* **2009**, *11*, 2685–2700. [[CrossRef](#)] [[PubMed](#)]
5. Rahal, A.; Kumar, A.; Singh, V.; Yadav, B.; Tiwari, R.; Chakraborty, S.; Dhama, K. Oxidative stress, prooxidants, and antioxidants: The interplay. *BioMed. Res. Int.* **2014**, 1–19. [[CrossRef](#)] [[PubMed](#)]
6. Evans, M.D.; Dizdaroglu, M.; Cooke, M.S. Oxidative DNA damage and disease: Induction, repair and significant. *Mutat. Res. Rev. Mutat. Res.* **2004**, *567*, 1–61. [[CrossRef](#)] [[PubMed](#)]
7. Fiorani, M.; Cantoni, O.; Tasinato, A.; Boscoboinik, D.; Azzi, A. Hydrogen peroxide-and fetal bovine serum-induced DNA synthesis in vascular smooth muscle cells: Positive and negative regulation by protein kinase C isoforms. *BBA Mol. Cell Res.* **1995**, *1269*, 98–104. [[CrossRef](#)]
8. Ahmed, A.F.; Attia, F.A.K.; Liu, Z.; Li, C.; Wei, J.; Kang, W. Antioxidant activity and total phenolic content of essential oils and extracts of sweet basil *Ocimum basilicum* L. plants. *Food Sci. Hum. Wellness* **2019**, *8*, 299–305. [[CrossRef](#)]
9. Derakhshan, Z.; Ferrante, M.; Tadi, M.; Ansari, F.; Heydari, A.; Hosseini, M.S.; Conti, G.O.; Sadrabad, E.K. Antioxidant activity and total phenolic content of ethanolic extract of pomegranate peels, juice and seeds. *Food Chem. Toxicol.* **2018**, *114*, 108–111. [[CrossRef](#)]
10. Ayoub, I.M.; El-Shazly, M.; Lu, M.-C.; Singab, A.N.B. Antimicrobial and cytotoxic activities of the crude extracts of *Dietes bicolor* leaves, flowers and rhizomes. *S. Afr. J. Bot.* **2014**, *95*, 97–101. [[CrossRef](#)]
11. Baena Ruiz, R.; Salinas Hernández, P. Cancer chemoprevention by dietary phytochemicals: Epidemiological evidence. *Maturitas* **2016**, *94*, 13–19. [[CrossRef](#)] [[PubMed](#)]
12. Saleh, A.S.M.; Wang, P.; Wang, N.; Yang, L.; Xiao, Z. Brown rice versus white rice: Nutritional quality, potential health benefits, development of food products, and preservation technologies. *Compr. Rev. Food Sci. Food Saf.* **2019**, *18*, 1070–1096. [[CrossRef](#)]
13. Blancquaert, D.; Van Daele, J.; Strobbe, S.; Kiekens, F.; Storozhenko, S.; De Steur, H.; Gellynck, X.; Lambert, W.; Stove, C.; Van Der Straeten, D. Improving folate (vitamin B9) stability in biofortified rice through metabolic engineering. *Nat. Biotechnol.* **2015**, *33*, 1076–1078. [[CrossRef](#)]
14. Zhu, Q.; Zeng, D.; Yu, S.; Cui, C.; Li, J.; Li, H.; Chen, J.; Zhang, R.; Zhao, X.; Chen, L.; et al. From golden rice to aSTARice: Bioengineering astaxanthin biosynthesis in rice endosperm. *Mol Plant.* **2018**, *11*, 1440–1448. [[CrossRef](#)] [[PubMed](#)]
15. Au, K.S.; Findley, T.O.; Northrup, H. Finding the genetic mechanisms of folate deficiency and neural tube defects-leaving no stone unturned. *Am. J. Med. Genet.* **2017**, *173*, 3042–3057. [[CrossRef](#)] [[PubMed](#)]
16. Socha, D.S.; DeSouza, S.I.; Flagg, A.; Sekeres, M.; Rogers, H.J. Severe megaloblastic anemia: Vitamin deficiency and other causes. *Cleve Clin J. Med.* **2020**, *87*, 153–164. [[CrossRef](#)] [[PubMed](#)]
17. Long, P.; Liu, X.; Li, J.; He, S.; Chen, H.; Yuan, Y.; Qiu, G.; Yu, K.; Liu, K.; Jiang, J.; et al. Circulating folate concentrations and risk of coronary artery disease: A prospective cohort study in Chinese adults and a Mendelian randomization analysis. *Am. J. Clin. Nutr.* **2020**, *111*, 635–643. [[CrossRef](#)]
18. Corrada, M.M.; Kawas, C.H.; Hallfrisch, J.; Muller, D.; Brookmeyer, R. Reduced risk of Alzheimer's disease with high folate intake: The Baltimore Longitudinal Study of Aging. *Alzheimers. Dement.* **2005**, *1*, 11–18. [[CrossRef](#)]
19. Agodi, A.; Barchitta, M.; Quattrocchi, A.; Maugeri, A.; Canto, C.; Marchese, A.E.; Vinciguerra, M. Low fruit consumption and folate deficiency are associated with LINE-1 hypomethylation in women of a cancer-free population. *Genes Nutr.* **2015**, *10*, 30. [[CrossRef](#)]
20. Punshon, T.; Carey, A.-M.; Ricachenevsky, F.K.; Meharg, A.A. Elemental distribution in developing rice grains and the effect of flag-leaf arsenate exposure. *Environ. Exp. Bot.* **2018**, *149*, 51–58. [[CrossRef](#)]
21. Luo, H.; He, L.; Du, B.; Pan, S.; Mo, Z.; Duan, M.; Tian, H.; Tang, X. Biofortification with chelating selenium in fragrant rice: Effects on photosynthetic rates, aroma, grain quality and yield formation. *Field Crop. Res.* **2020**, *255*, 107909. [[CrossRef](#)]
22. Zaynab, M.; Fatima, M.; Abbas, S.; Sharif, Y.; Umair, M.; Zafar, M.H.; Bahadar, K. Role of secondary metabolites in plant defense against pathogens. *Microb. Pathog.* **2018**, *124*, 198–202. [[CrossRef](#)] [[PubMed](#)]
23. Kaur, M.; Asthir, B.; Mahajan, G. Variation in antioxidants, bioactive compounds and antioxidant capacity in germinated and ungerminated grains of ten rice cultivars. *Rice Sci.* **2017**, *24*, 349–359. [[CrossRef](#)]

24. Tamprasit, K.; Weerapreeyakul, N.; Sutthanut, K.; Thukhammee, W.; Wattanathorn, J. Harvest age effect on phytochemical content of white and black glutinous rice cultivars. *Molecules* **2019**, *24*, 4432. [[CrossRef](#)]
25. Khaleghnezhad, V.; Yousefi, A.R.; Tavakoli, A.; Farajmand, B. Interactive effects of abscisic acid and temperature on rosmarinic acid, total phenolic compounds, anthocyanin, carotenoid and flavonoid content of dragonhead (*Dracocephalum moldavica* L.). *Sci. Hort.* **2019**, *250*, 302–309. [[CrossRef](#)]
26. Agbor, G.A.; Vinson, J.A.; Donnelly, P.E. Folin-Ciocalteu reagent for polyphenolic assay. *Int. J. Food Sci. Nutr. Diet.* **2014**, *8*, 147–156. [[CrossRef](#)]
27. Khandhapok, P.; Muangprom, A.; Sukrong, S. Antioxidant activity and DNA protective properties of rice grass juices. *Sci. Asia* **2015**, *41*, 119. [[CrossRef](#)]
28. Lee, J.; Durst, R.W.; Wrolstad, R.E. Determination of total monomeric anthocyanin pigment content of fruit juices, beverages, natural colorants, and wines by the pH differential method: Collaborative study. *J. AOAC Int.* **2005**, *88*, 10. [[CrossRef](#)]
29. Fuleki, T.; Francis, F.J. Quantitative methods for anthocyanins. 1. Extraction and determination of total anthocyanin in cranberries. *J. Food Sci.* **1968**, *33*, 72–77. [[CrossRef](#)]
30. Al-Qassabi, J.S.A.; Weli, A.M.; Hossain, M.A. Comparison of total phenols content and antioxidant potential of peel extracts of local and imported lemons samples. *Sustain. Chem. Pharm.* **2018**, *8*, 71–75. [[CrossRef](#)]
31. Nimse, S.B.; Pal, D. Free radicals, natural antioxidants, and their reaction mechanisms. *Rsc Adv.* **2015**, *5*, 27986–28006. [[CrossRef](#)]
32. Khamphio, M.; Barusrux, S.; Weerapreeyakul, N. Sesamol induces mitochondrial apoptosis pathway in HCT116 human colon cancer cells via pro-oxidant effect. *Life Sci.* **2016**, *158*, 46–56. [[CrossRef](#)] [[PubMed](#)]
33. Machana, S.; Weerapreeyakul, N.; Barusrux, S.; Nonpunya, A.; Sripanidkulchai, B.; Thitimetharoch, T. Cytotoxic and apoptotic effects of six herbal plants against the human hepatocarcinoma (HepG2) cell line. *Chin. Med.* **2011**, *6*, 39. [[CrossRef](#)] [[PubMed](#)]
34. Prayong, P.; Barusrux, S.; Weerapreeyakul, N. Cytotoxic activity screening of some indigenous Thai plants. *Fitoterapia* **2008**, *79*, 598–601. [[CrossRef](#)]
35. Sangthong, S.; Weerapreeyakul, N. Simultaneous quantification of sulforaphene and sulforaphane by reverse phase HPLC and their content in *Raphanus sativus* L. var. *caudatus* Alef extracts. *Food Chem.* **2016**, *201*, 139–144. [[CrossRef](#)]
36. Pocasap, P.; Weerapreeyakul, N.; Thumanu, K. Alyssin and iberin in cruciferous vegetables exert anticancer activity in HepG2 by increasing intracellular reactive oxygen species and tubulin depolymerization. *Biomol. Ther.* **2019**, *27*, 540–552. [[CrossRef](#)]
37. Gerl, R. Apoptosis in the development and treatment of cancer. *Carcinogenesis* **2004**, *26*, 263–270. [[CrossRef](#)]
38. Zhang, C.; Li, F.; Li, J.; Xu, Y.; Wang, L.; Zhang, Y. Docetaxel down-regulates PD-1 expression via STAT3 in T lymphocytes. *Clin. Lung Cancer* **2018**, *19*, e675–e683. [[CrossRef](#)]
39. Dhakshinamoorthy, S.; Dinh, N.-T.; Skolnick, J.; Styczynski, M.P. Metabolomics identifies the intersection of phosphoethanolamine with menaquinone-triggered apoptosis in an *in vitro* model of leukemia. *Mol. Biosyst.* **2015**, *11*, 2406–2416. [[CrossRef](#)]
40. Si, M.-S.; Imagawa, D.K.; Ji, P.; Wei, X.; Holm, B.; Kwok, J.; Lee, M.; Reitz, B.A.; Borie, D.C. Immunomodulatory effects of docetaxel on human lymphocytes. *Invest. New Drugs* **2003**, *21*, 281–290. [[CrossRef](#)]
41. Amarowicz, R.; Pegg, R.B. Natural antioxidants of plant origin. *Adv. Food Nutr. Res.* **2019**, *90*, 1–81. [[PubMed](#)]
42. Alam, M.N.; Bristi, N.J.; Rafiquzzaman, M. Review on *in vivo* and *in vitro* methods evaluation of antioxidant activity. *Saudi Pharm. J.* **2013**, *21*, 143–152. [[CrossRef](#)] [[PubMed](#)]
43. Hidayat, M.A.; Fitri, A.; Kuswandi, B. Scanometry as microplate reader for high throughput method based on DPPH dry reagent for antioxidant assay. *Acta Pharm. Sin. B* **2017**, *7*, 395–400. [[CrossRef](#)] [[PubMed](#)]
44. Liang, N.; Kitts, D. Antioxidant property of coffee components: Assessment of methods that define mechanisms of action. *Molecules* **2014**, *19*, 19180–19208. [[CrossRef](#)]
45. Birben, E.; Sahiner, U.M.; Sackesen, C.; Erzurum, S.; Kalayci, O. Oxidative stress and antioxidant defense. *World Allergy Organ. J.* **2012**, *5*, 9–19. [[CrossRef](#)] [[PubMed](#)]
46. Bridge, G.; Rashid, S.; Martin, S.A. DNA mismatch repair and oxidative DNA damage: Implications for cancer biology and treatment. *Cancers* **2014**, *6*, 1597–1614. [[CrossRef](#)]
47. Sosa, V.; Moliné, T.; Somoza, R.; Paciucci, R.; Kondoh, H.; LLeonart, M.E. Oxidative stress and cancer: An overview. *Ageing Res. Rev.* **2013**, *12*, 376–390. [[CrossRef](#)]

48. Lewandowska, U.; Gorlach, S.; Owczarek, K.; Hrabec, E.; Szewczyk, K. Synergistic interactions between anticancer chemotherapeutics and phenolic compounds and anticancer synergy between polyphenols. *Postepy Hig. Med. Dosw.* **2014**, *13*, 528–540. [[CrossRef](#)]
49. Pham, H.N.T.; Sakoff, J.A.; Vuong, Q.V.; Bowyer, M.C.; Scarlett, C.J. Screening phytochemical content, antioxidant, antimicrobial and cytotoxic activities of *Catharanthus roseus* (L.) G. Don stem extract and its fractions. *Biocatal. Agric. Biotechnol.* **2018**, *16*, 405–411. [[CrossRef](#)]
50. Deepika, S.; Selvaraj, C.I.; Roopan, S.M. Screening bioactivities of *Caesalpinia pulcherrima* L. swartz and cytotoxicity of extract synthesized silver nanoparticles on HCT116 cell line. *Mater. Sci. Eng. C* **2020**, *106*, 110279. [[CrossRef](#)]
51. Mu, W.; Liu, L.-Z. Reactive oxygen species signaling in cancer development. *React. Oxyg. Species* **2017**, *4*, 251–265. [[CrossRef](#)]
52. Matt, S.; Hofmann, T.G. The DNA damage-induced cell death response: A roadmap to kill cancer cells. *Cell. Mol. Life Sci.* **2016**, *73*, 2829–2850. [[CrossRef](#)] [[PubMed](#)]
53. Kaina, B. DNA damage-triggered apoptosis: Critical role of DNA repair, double-strand breaks, cell proliferation and signaling. *Biochem. Pharmacol.* **2003**, *66*, 1547–1554. [[CrossRef](#)]
54. Aljuhani, N.; Ismail, R.S.; El-Awady, M.S.; Hassan, M.H. Modulatory effects of perindopril on cisplatin-induced nephrotoxicity in mice: Implication of inflammatory cytokines and caspase-3 mediated apoptosis. *Acta Pharm.* **2020**, *70*, 515–525. [[CrossRef](#)] [[PubMed](#)]
55. Pistritto, G.; Trisciuglio, D.; Ceci, C.; Garufi, A.; D’Orazi, G. Apoptosis as anticancer mechanism: Function and dysfunction of its modulators and targeted therapeutic strategies. *Aging* **2016**, *8*, 603–619. [[CrossRef](#)] [[PubMed](#)]
56. Vince, J.E.; De Nardo, D.; Gao, W.; Vince, A.J.; Hall, C.; McArthur, K.; Simpson, D.; Vijayaraj, S.; Lindqvist, L.M.; Bouillet, P.; et al. The mitochondrial apoptotic effectors BAX/BAK activate caspase-3 and -7 to trigger NLRP3 inflammasome and caspase-8 driven IL-1 β activation. *Cell Rep.* **2018**, *25*, 2339–2353. [[CrossRef](#)] [[PubMed](#)]
57. Horie, Y.; Nemoto, H.; Itoh, M.; Kosaka, H.; Morita, K. Fermented brown rice extract causes apoptotic death of human acute lymphoblastic leukemia cells via death receptor pathway. *Appl. Biochem. Biotechnol.* **2016**, *178*, 1599–1611. [[CrossRef](#)]
58. Redza-Dutordoir, M.; Averill-Bates, D.A. Activation of apoptosis signalling pathways by reactive oxygen species. *BBA Mol. Cell Res.* **2016**, *1863*, 2977–2992. [[CrossRef](#)]
59. Cordier, W.; Steenkamp, P.; Steenkamp, V. Extracts of *Moringa oleifera* lack cytotoxicity and attenuate oleic acid-induced steatosis in an *in vitro* HepG2 model. *S. Afr. J. Bot.* **2019**, S0254629919301607. [[CrossRef](#)]
60. Walle, T. Methylation of dietary flavones increases their metabolic stability and chemopreventive effects. *Int. J. Mol. Sci.* **2009**, *10*, 5002–5019. [[CrossRef](#)]
61. Park, E.-J.; Pezzuto, J.M. Flavonoids in cancer prevention. *Anti Cancer Agents Med. Chem.* **2012**, *12*, 836–851. [[CrossRef](#)] [[PubMed](#)]



© 2020 by the authors. Licensee MDPI, Basel, Switzerland. This article is an open access article distributed under the terms and conditions of the Creative Commons Attribution (CC BY) license (<http://creativecommons.org/licenses/by/4.0/>).